Supplementary Information

Photoresponsive Hydrogel Friction

Allison L. Chau[a*], Kseniia M. Karnaukh[b*], Ian Maskiewicz[b], Javier Read de Alaniz[b], and Angela A. Pitenis[a]

[a]Materials Department
[b]Department of Chemistry and Biochemistry
University of California, Santa Barbara, Santa Barbara, CA, United States
*equal contribution

Corresponding Authors:
Javier Read de Alaniz
javier@chem.ucsb.edu

Angela A. Pitenis
apitenis@ucsb.edu

1.0 Synthesis & Chemical Characterization Methoxy-Spiropyran-Methacrylate

1.1 Chemical Characterization

Solvents and reagents were purchased from commercial vendors and used without further purification unless otherwise specified. Anhydrous methanol (MeOH) was purchased from Sigma Aldrich. Acetonitrile (CH_3CN) for reactions was dispensed from a solvent purification system. Ethanol (EtOH) was stored over 3Å molecular sieves.

Thin-layer chromatography (TLC) was carried out with Merck TLC plates (silica gel 60 F254 on aluminum) and visualized by exposure to UV light (254/ 366 nm). Silica gel chromatography was performed using silica gel (60 Å pore size, 40 – 63 μm particle size). ^1H and ^{13}C NMR spectra were recorded at 298 K on a Bruker Avance III HD 400 MHz or a Bruker Avance NEO 500 MHz NMR spectrometer using $CDCl_3$ or DMSO-d_6 as the solvent. Chemical shifts (δ) are reported relative to residual solvent peaks (δ 7.26 ppm for $CDCl_3$ and 2.50 ppm for DMSO-d_6 in ^1H NMR; δ 77.16 for $CDCl_3$ and 39.52 ppm for DMSO-d_6 in ^{13}C NMR). Mass spectral data was collected on the Shimadzu LCMS-9030 Q-TOF Mass Spectrometer with an electrospray ionization (ESI) source.

1.2 Synthesis of 5-methoxy-2,3,3-trimethyl-3H-indole

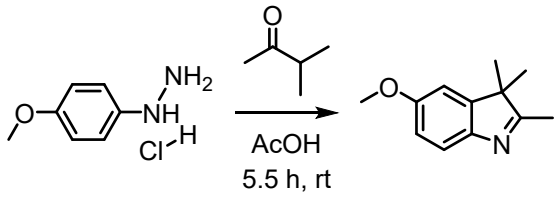

Synthesis of 5-methoxy-2,3,3-trimethyl-3*H*-indole was adapted from Wimberger *et al.*[1] To a solution of 3-methyl-2-butanone (7.53 mL, 6.05 g, 70.2 mmol, 2 eq.) in 150 mL glacial acetic acid, 4-methoxyphenylhydrazine hydrochloride (6.13 g, 35.1 mmol, 1 eq.) was added. The suspension was heated to 150 °C for 20 min to dissolve starting materials, resulting in a color change from colorless to dark purple. The mixture was then stirred at room temperature overnight, followed by the slow addition of potassium hydroxide pellets to neutralize the reaction mixture. The solution was extracted with diethyl ether (3×100 mL), and the combined organic phases were washed with brine (2×75 mL), dried over $MgSO_4$, and concentrated under reduced pressure. If necessary, the final product can be purified by column chromatography (hex/EtOAc = 7/3 → 1/1). Due to possible decomposition at room temperature, the product was kept in the fridge (4.98 g, 26.3 mmol, 75% yield).

^{1}H NMR (400 MHz, $CDCl_3$) δ (ppm): 7.41 (dd, *J* = 8.2, 0.7 Hz, 1H), 6.87 – 6.78 (m, 2H), 3.83 (s, 3H), 2.24 (s, 3H), 1.28 (s, 6H).

Spectral data matches those reported in the literature.[1]

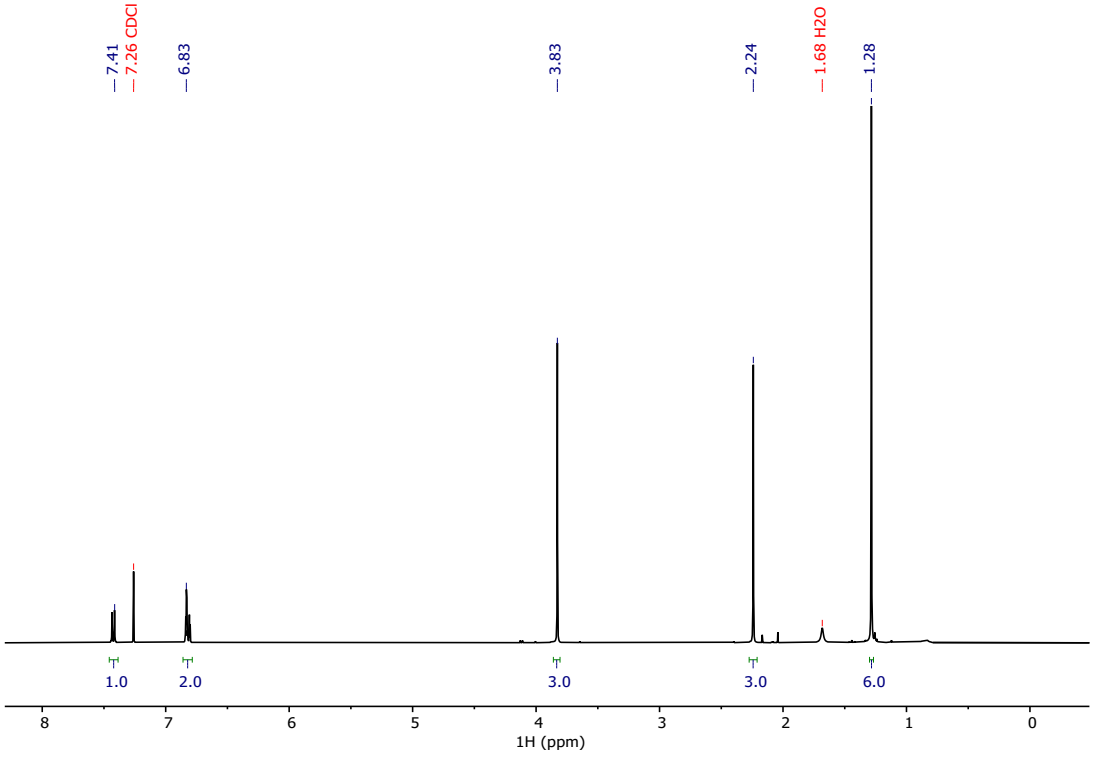

Figure S1. ^{1}H NMR spectrum of 5-methoxy-2,3,3-trimethyl-3*H*-indole.

1.3 Synthesis of 1-(2-hydroxyethyl)-2,3,3-trimethyl-3*H*-indolium bromide

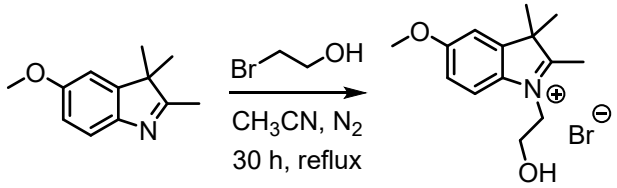

Synthesis of 1-(2-hydroxyethyl)-2,3,3-trimethyl-3*H*-indolium bromide was adapted and modified from Stupp *et al*.[2] To an oven-dry round bottom flask equipped with a magnetic stir bar and condenser was added 5-methoxy-2,3,3-trimethyl-3*H*-indole (5.17 g, 27.3 mmol, 1 eq.) and of 2-bromoethanol (6.82 g, 54.6 mmol, 2 eq.) in 80 mL of absolute acetonitrile, followed by solution nitrogen bubbling for 10 minutes. The solution was refluxed under a nitrogen atmosphere for 30 h at 85 °C to ensure complete conversion. Upon completion, the mixture was cooled to room temperature, and acetonitrile was removed under reduced pressure. Ensure complete removal of acetonitrile for efficient extraction. The product was redissolved in 100 mL of dichloromethane (DCM) and extracted with DI water (3×100 mL). The aqueous phase was collected, after which the final solution was subjected to rotary evaporation at 60 °C, followed by drying in a vacuum oven to get the reddish-colored product (6.4 g, 20.48 mmol, 75% yield).

^{1}H NMR (500 MHz, DMSO-d$_6$) δ (ppm): 7.87 (d, *J* = 8.8 Hz, 1H), 7.50 (d, *J* = 2.5 Hz, 1H), 7.13 (dd, *J* = 8.9, 2.5 Hz, 1H), 4.56 (t, *J* = 5.1 Hz, 2H), 3.86 (s, 3H), 3.84 (d, *J* = 4.3 Hz, 2H), 2.76 (s, 3H), 1.53 (s, 6H).

^{13}C NMR (126 MHz, DMSO-d$_6$) δ (ppm): 194.77, 160.53, 143.90, 134.34, 116.55, 114.21, 109.35, 57.83, 56.12, 54.04, 50.30, 22.11, 14.19.

LC-MS (ESI) (m/z): $[M]^+$ calculated for $C_{14}H_{20}NO_2^+$: 234.1494, found: 234.1497.

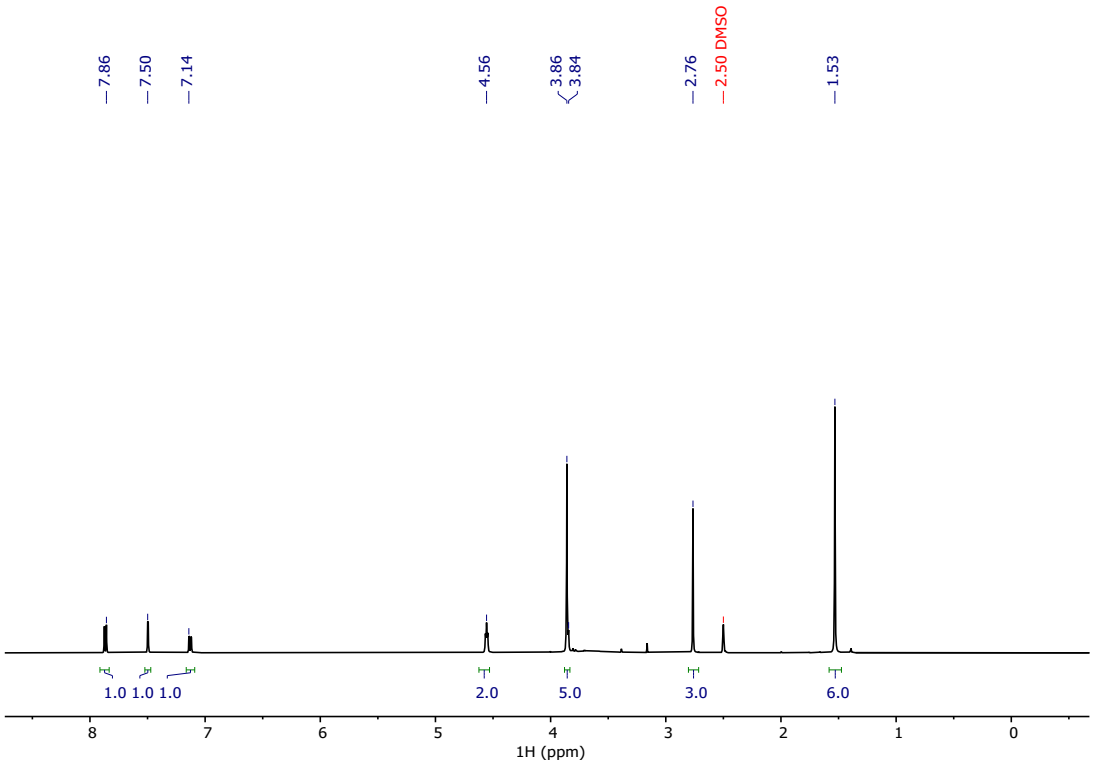

Figure S2. ^{1}H NMR spectrum of 1-(2-hydroxyethyl)-2,3,3-trimethyl-3*H*-indolium bromide.

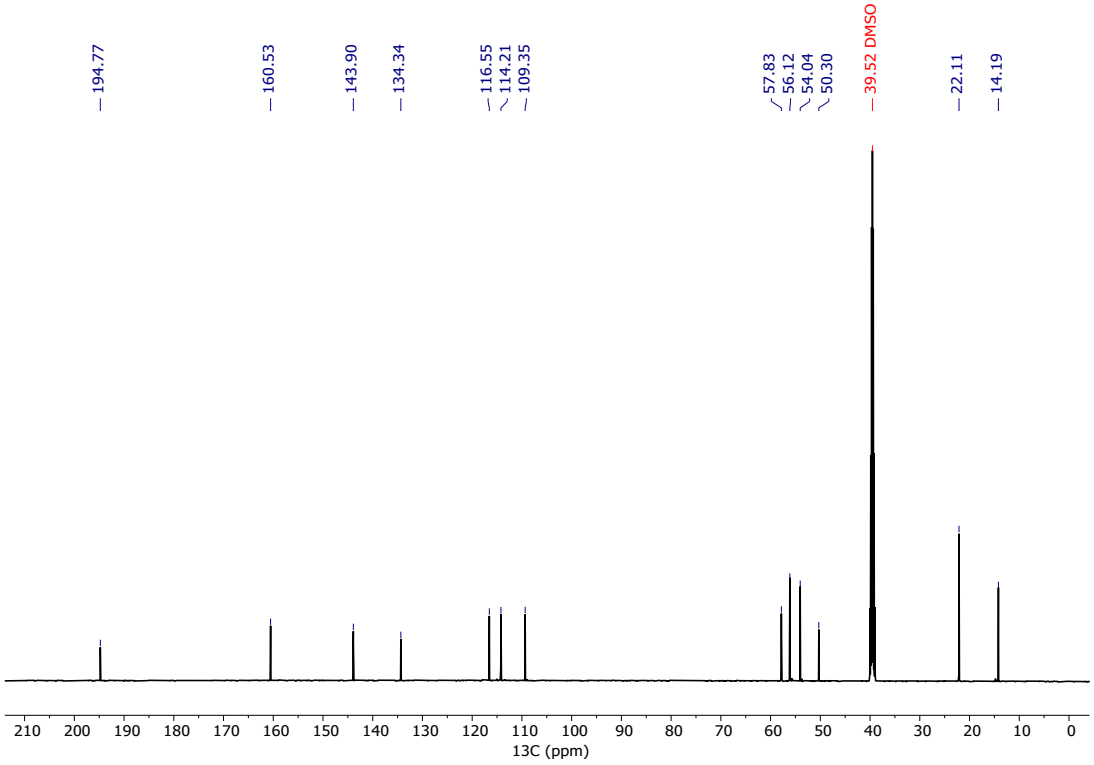

Figure S3. ^{13}C NMR spectrum of 1-(2-hydroxyethyl)-2,3,3-trimethyl-3*H*-indolium bromide.

1.4 Synthesis of **2-(5'-methoxy-3',3'-dimethylspiro[chromene-2,2'-indolin]-1'-yl)ethan-1-ol**

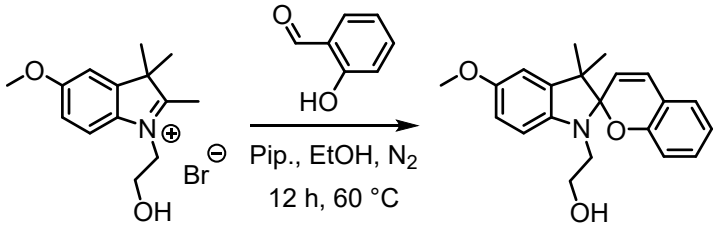

The synthesis of 2-(5'-methoxy-3',3'-dimethylspiro[chromene-2,2'-indolin]-1'-yl)ethan-1-ol was adapted and modified from Stupp *et al*.[2] To an oven-dry three-neck round-bottom flask equipped with a magnetic stir bar and air condenser, salicylaldehyde (1.4 g, 11.46 mmol, 1.2 eq.) was added to a solution of 1-(2-hydroxyethyl)-2,3,3-trimethyl-3*H*-indolium bromide (3.0 g, 9.55 mmol, 1 eq.) in 70 mL of anhydrous ethanol under nitrogen atmosphere. The solution was heated to 60 °C, after which piperidine (1.13 mL, 0.98 g, 11.46 mmol, 1.2 eq.) was added, and the reaction proceeded for 12 hours under an inert atmosphere. Upon completion, the mixture was cooled to room temperature, and the solvent was removed under reduced pressure. The crude product was redissolved in DCM and purified by column chromatography (DCM/MeOH = 100/0 → 97/3). (2.74 g, 8.12 mmol, 85% yield).

^{1}H NMR (500 MHz, $CDCl_3$) δ (ppm): 7.09 (ddd, *J* = 8.8, 7.5, 1.7 Hz, 1H), 7.03 (dd, *J* = 7.5, 1.7 Hz, 1H), 6.84 – 6.80 (m, 2H), 6.74 – 6.65 (m, 3H), 6.54 (d, *J* = 8.3 Hz, 1H), 5.67 (d, *J* = 10.2 Hz, 1H), 3.79 (s, 3H), 3.77 – 3.69 (m, 2H), 3.46 (ddd, *J* = 14.9, 7.4, 5.1 Hz, 1H), 3.26 (dt, *J* = 14.8, 5.0 Hz, 1H), 1.93 (t, *J* = 6.3 Hz, 1H), 1.29 (s, 3H), 1.17 (s, 3H).

^{13}C NMR (126 MHz, $CDCl_3$) δ (ppm): 154.09, 154.03, 141.78, 138.29, 129.99, 129.63, 126.95, 120.48, 119.68, 118.74, 115.15, 111.29, 109.99, 106.85, 105.14, 60.99, 56.07, 52.56, 46.66, 25.87, 20.36.

LC-MS (ESI) (m/z): $[M+H]^+$ calculated for $C_{21}H_{23}NO_3$ is 338.1756, found: 338.1762.

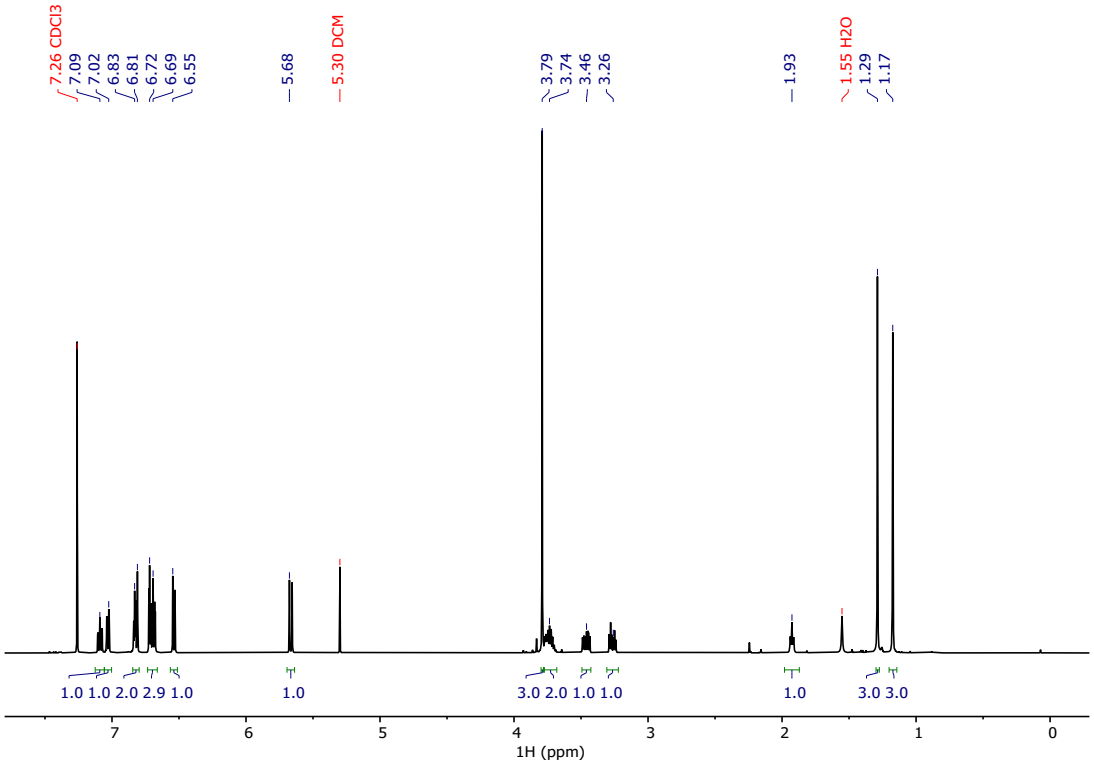

Figure S4. ^{1}H NMR spectrum of 2-(5'-methoxy-3',3'-dimethylspiro[chromene-2,2'-indolin]-1'-yl)ethan-1-ol.

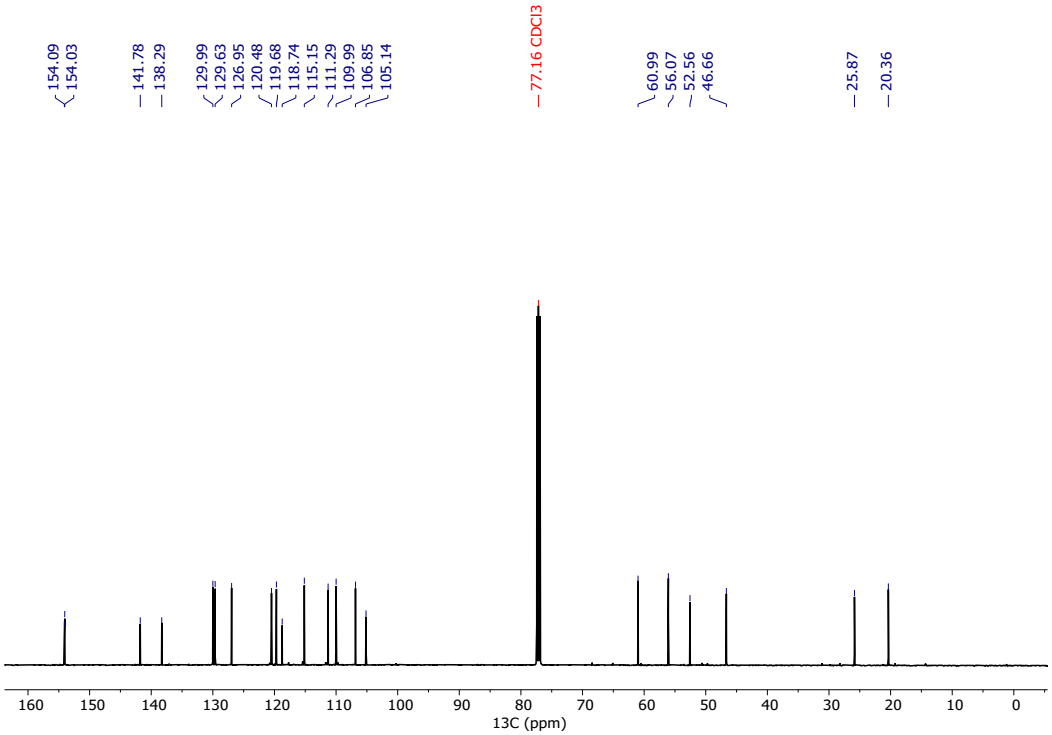

Figure S5. ^{13}C NMR spectrum of 2-(5'-methoxy-3',3'-dimethylspiro[chromene-2,2'-indolin]-1'-yl)ethan-1-ol.

1.5 Synthesis of 2-(5'-methoxy-3',3'-dimethylspiro[chromene-2,2'-indolin]-1'-yl)ethyl methacrylate (methoxy-spiropyran-methacrylate) (methoxy-SP-MA)

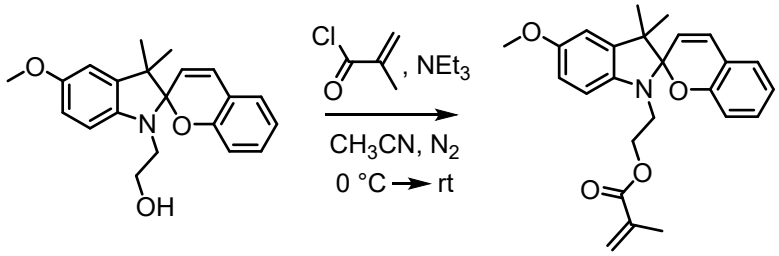

The synthesis of 2-(5'-methoxy-3',3'-dimethylspiro[chromene-2,2'-indolin]-1'-yl)ethyl methacrylate was adapted and modified from Stupp *et al*.[2] To a round bottom flask equipped with a magnetic stir bar and condenser, 2-(5'-methoxy-3',3'-dimethylspiro[chromene-2,2'-indolin]-1'-yl)ethan-1-ol (1.8 g, 5.33 mmol, 1 eq.) was added to 70 mL of anhydrous acetonitrile, followed by the addition of triethylamine (1.19 g, 11.73 mmol, 2.2 eq.) under nitrogen atmosphere. The reaction mixture was cooled to 0 °C followed by a drop-wise addition of methacryloyl chloride (1.23 g, 11.73 mmol, 2.2 eq.), pre-dissolved in 10 mL of absolute acetonitrile. The reaction was stirred for 1 hour at 0 °C, after which the reaction proceeded at room temperature overnight. The solvent was removed under reduced pressure, and the crude product was purified by column chromatography (DCM/MeOH = 100/0 → 95/5). (1.69 g, 4.16 mmol, 78% yield).

^{1}H NMR (500 MHz, $CDCl_3$) δ (ppm): 7.12 – 7.06 (m, 1H), 7.04 (d, *J* = 7.4 Hz, 1H), 6.85 – 6.80 (m, 2H), 6.74 – 6.67 (m, 3H), 6.59 (d, *J* = 8.1 Hz, 1H), 6.10 (s, 1H), 5.68 (d, *J* = 10.2 Hz, 1H), 5.56 (s, 1H), 4.30 (t, *J* = 6.8 Hz, 2H), 3.80 (s, 3H), 3.57 (dt, *J* = 14.1, 6.7 Hz, 1H), 3.34 (dt, *J* = 15.0, 6.0 Hz, 1H), 1.94 (s, 3H), 1.29 (s, 4H), 1.16 (s, 3H).

^{13}C NMR (126 MHz, $CDCl_3$) δ (ppm): 167.44, 154.30, 153.93, 141.65, 138.14, 136.33, 129.91, 129.54, 126.90, 125.81, 120.26, 119.70, 118.63, 115.18, 111.31, 109.87, 106.60, 105.05, 63.20, 56.05, 52.54, 42.93, 25.85, 20.10, 18.51.

LC-MS (ESI) (m/z): $[M+H]^+$ calculated for $C_{25}H_{27}NO_4$ is 406.2018, $[M+H]^+$ found: 406.2025.

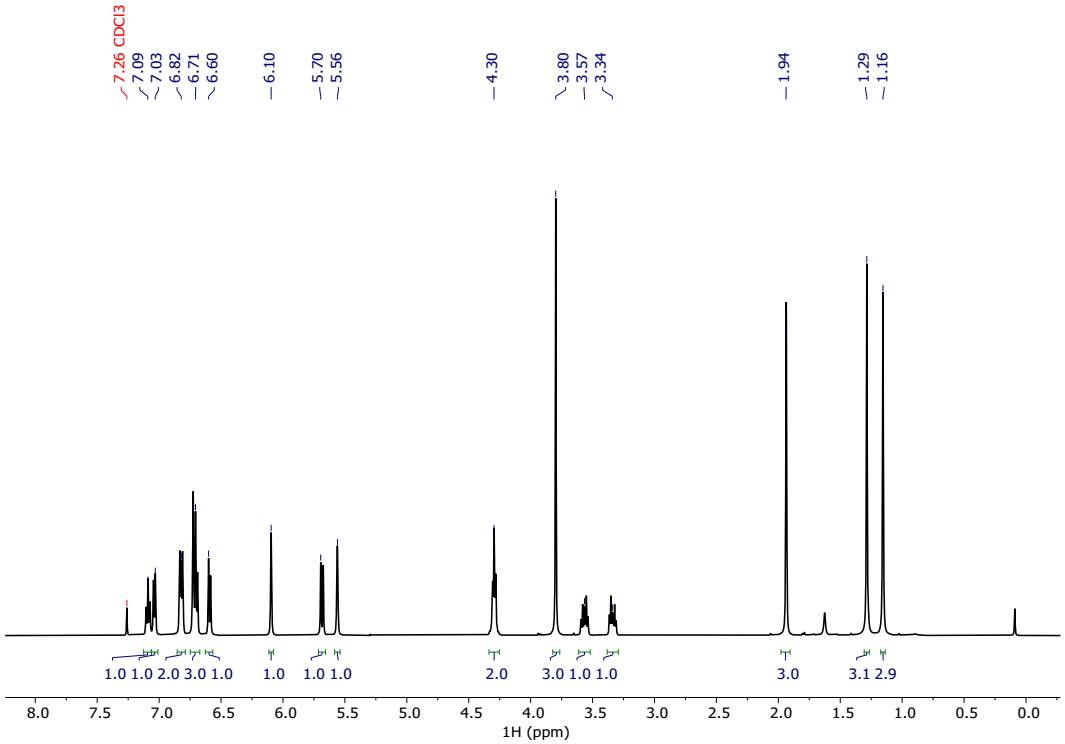

Figure S6. [1]H NMR spectrum of 2-(5'-methoxy-3',3'-dimethylspiro[chromene-2,2'-indolin]-1'-yl)ethyl methacrylate.

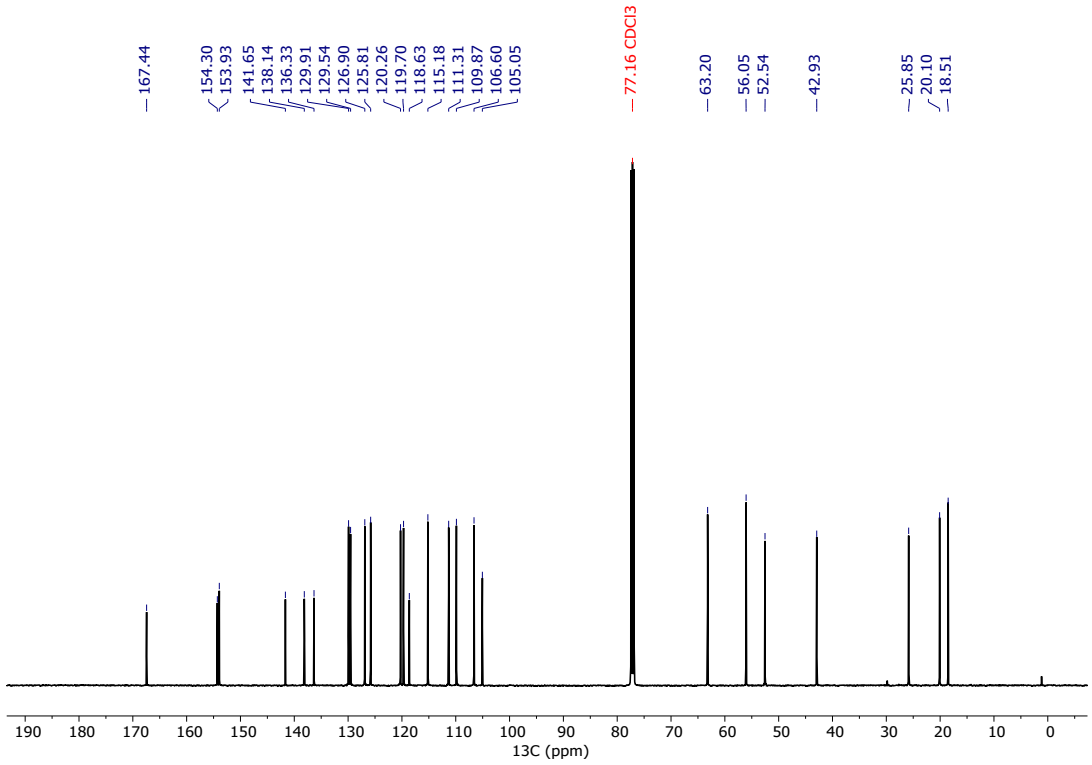

Figure S7. [13]C NMR spectrum of 2-(5'-methoxy-3',3'-dimethylspiro[chromene-2,2'-indolin]-1'-yl)ethyl methacrylate.

2.0 UV-Vis Spectroscopy

2.1 Time-dependent UV-Vis Spectroscopy

The photoinduced optical absorption kinetics was measured on a home-built pump-probe setup, as previously reported by our group.[3] The blue pump beam was generated by a light-emitting diode (LED) source (Thorlabs, Inc. M470F3) coupled into a multimode optical fiber terminated with an output collimator (I = 25 ± 1 mW/cm^2). The LED intensity was controlled through a digital-to-analog converter (National Instruments USB-6009) using LabVIEW. The probe beam was generated by an incandescent light bulb source (Ocean Optics LS1) coupled into a multimode fiber with an output collimator for light delivery. The probe light was modulated by a shutter (Uniblitz CS25), which could be controlled manually or through a digital output port (National Instruments USB-6009) using LabVIEW. Pump and probe beams overlapped using steering and focusing optics at a 90° angle inside a sample holder, allowing 10×10 mm^2 rectangular spectrophotometer cells to be held within or cast film samples to be held to the front using metal spring clips. The solutions were continuously stirred during the measurements by a miniature stirring plate inserted into the sample holder (Starna Cells SCS 1.11). Both pump and probe beams were nearly collimated inside the cell with a diameter of about 2 mm. The pump beam was blocked after passing through the sample, and the probe beam was directed by a system of lenses into the detector (Ocean Optics Flame-S1-XR spectrometer), which acquired spectra of the probe light. The detector was connected to a PC via a USB port. The experiment was controlled by a National Instrument LabVIEW program, which collected the probe light spectra, determined sample optical absorption spectra, and controlled pump and probe light sources.

2.2 Acidification of Methanol

1.17 g (20 mmol) of NaCl was added to a 250 mL three-neck round-bottom flask equipped with an addition funnel and two rubber septa, followed by the slow addition of 1 ml of concentrated sulfuric acid. The HCl gas produced during the reaction was bubbled via a cannula into 100 mL of anhydrous MeOH solution in a round-bottom flask for 5 minutes. This flask was connected to an Erlenmeyer flask containing dilute sodium bicarbonate solution, which served as the trap for excess HCl gas. Ensure the cannula size is sufficient for efficient HCl gas exchange. To establish a consistent concentration of acid in methanol, the final "pH" of the MeOH was measured with a Thermo Scientific Orion Star™ A111 Benchtop pH Meter and then diluted with non-acidified anhydrous MeOH until a pH ≈ 2 was reached.

2.3 UV-Vis of Methoxy-Spiropyran-Methacrylate Monomer

Stock solution of methoxy-spiropyran-methacrylate (0.1 mM) was prepared by dissolving 2.03 mg (0.005 mmol) of monomer in 50 mL of acidified MeOH. The solution was wrapped in aluminum foil and stored at 4 °C. Prior to running UV-Vis experiments, the stock solution was diluted to a 0.02 mM concentration, transferred to a quartz cuvette with a 1 cm path length, placed in the spectrophotometer, and allowed to equilibrate thermally for 3 hours in the dark.

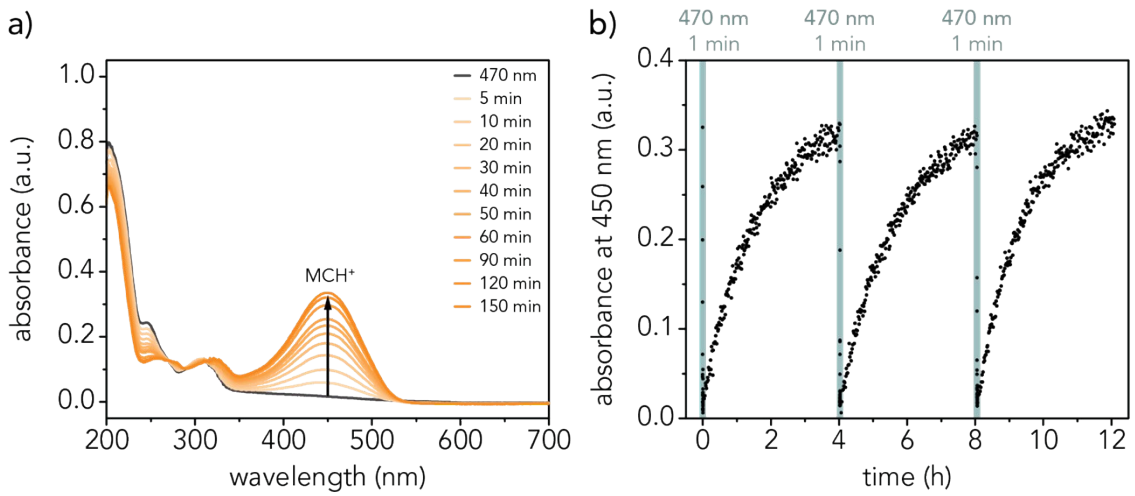

Figure S8 (a) UV-Vis spectra of 0.02 mM methoxy-spiropyran-methacrylate in acidified methanol (pH ≈ 2) across many time points. The absorbance at $\lambda \approx 450$ nm increased over time in the dark, indicating that the methoxy-SP-MA thermally relaxed from the SP to the MCH^+ form after 1 min of 470 nm irradiation. **(b)** Pump-probe kinetics measurements upon irradiation with 470 nm light (Thorlabs, Inc. M470F3). Absorbance over time monitored at $\lambda \approx 450$ nm absorbance peak demonstrates the switching kinetics between the two isomers. It takes ≈ 4 h to thermally relax from SP back to MCH^+ in the dark.

2.4 UV-Vis of Linear p(NIPAAm-*co*-AMPS-*co*-SP)

Linear p(NIPAAm-*co*-AMPS-*co*-SP) was synthesized following the method outlined in the main text in Section 2.3 but without adding the MBAm crosslinker and with greater AMPS concentration to ensure solubility of polymer in the phosphate buffer solution. 137 mg NIPAAm, 13.4 mg AMPS (5 mol.% relative to the total polymer concentration), and 13.1 mg methoxy-SP-MA (2.5 mol.%) was dissolved in a solution of 800 µL dioxane, 100 µL DI water, and 7.4 µL TEMED. The precursor was bubbled with nitrogen for 30 min, and then 100 µL of 10 wt.% APS was added to initiate polymerization. 10 mg of oven-dried linear polymer was added to 20 mL of 100 mM of phosphate buffer (pH ≈ 2) to obtain a 0.500 mg/mL stock solution. Prior to running UV-Vis experiments, the stock solution was diluted to 0.150 mg/mL concentration of the linear polymer, transferred to a quartz cuvette with 1 cm path length, placed in the spectrophotometer, and allowed to equilibrate thermally for 3 hours in the dark.

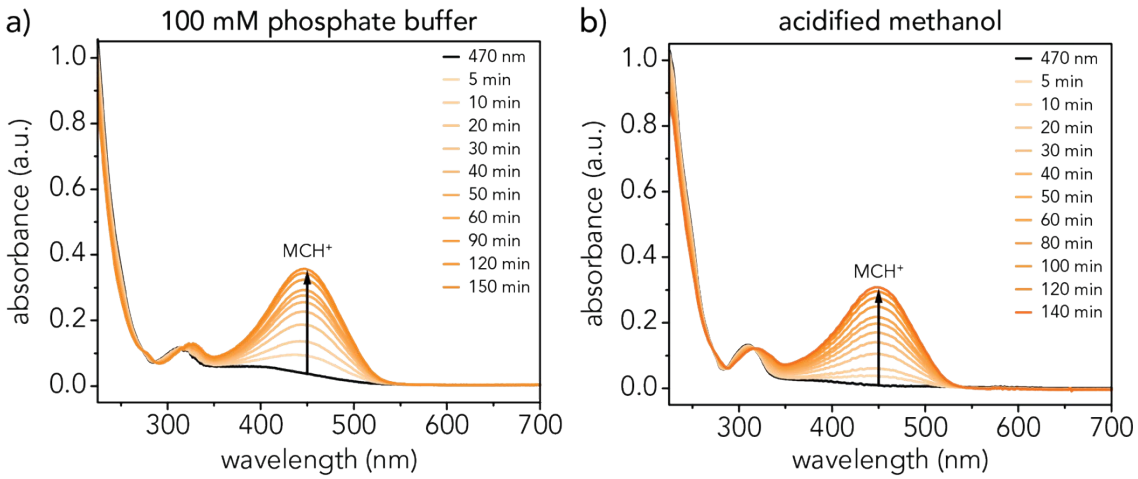

Figure S9 UV-Vis spectra of 0.150 mg/mL linear p(NIPAAm-*co*-AMPS-*co*-SP) in **(a)** 100 mM phosphate buffer (pH ≈ 2) and **(b)** acidified methanol (pH ≈ 2) across many time points. Similar to the methoxy-SP-MA monomers in solution (**Figure S8**), the absorbance at $\lambda \approx 450$ nm increased over time in the dark, indicating that the methoxy-SP-MA thermally relaxed from the SP conformation back to the MCH^+ conformation after 1 min of 470 nm irradiation.

2.5 UV-Vis of p(NIPAAm-*co*-AMPS-*co*-SP) *Hydrogel*

p(NIPAAm-*co*-AMPS-*co*-SP) hydrogel samples for UV-vis were prepared by dissolving 143 mg NIPAAm, 1.4 mg AMPS (0.5 mol.% relative to total polymer concentration), 2.7 mg methoxy-SP-MA (0.5 mol.%), and 5.1 mg of MBAm (0.5 mol.%) in a solution of 800 µL dioxane, 100 µL DI water, and 7.4 µL TEMED. The precursor solution was bubbled with nitrogen for 30 min. 100 µL of 10 wt.% APS was added (forming a 4:1 vol/vol solution of 1,4-dioxane:DI water) to initiate polymerization, and the precursor was polymerized between two glass slides with 0.4 mm thick Neoprene rubber spacers in a nitrogen-rich environment for 1 h while irradiated with 470 nm light.

The concentration of methoxy-SP-MA was decreased to 0.5 mol% for UV-Vis spectroscopy experiments compared to 2.5 mol% methoxy-SP-MA used for mechanical testing. Despite decreasing the methoxy-SP-MA concentration and hydrogel thickness, we still encountered challenges in characterization due to absorption oversaturation. Therefore, the switching kinetics between the two forms was monitored at $\lambda \approx 500$ nm absorbance peak.

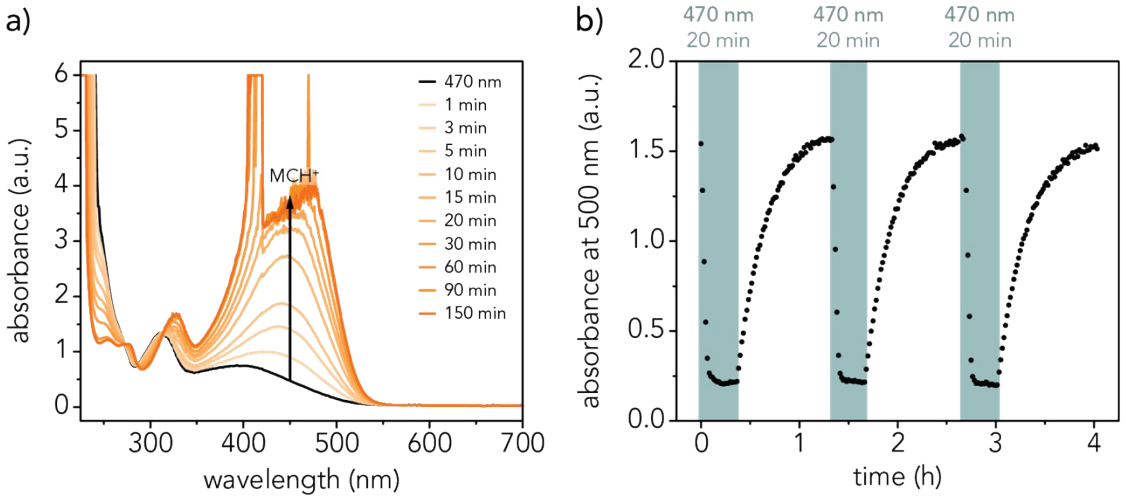

Figure S10 (a) UV-Vis spectra of p(NIPAAm-*co*-AMPS-*co*-SP) hydrogel with 0.5 mol.% methoxy-SP-MA in 100 mM phosphate buffer (pH ≈ 2) across several time points. The absorbance at $\lambda \approx 450$ nm increased over time in the dark, indicating that the methoxy-SP-MA thermally relaxed from the SP to the MCH^+ form after 1 min of 470 nm irradiation. **(b)** Pump-probe kinetics measurements upon irradiation with 470 nm light (Thorlabs, Inc. M470F3). Absorbance over time monitored at $\lambda \approx 500$ nm absorbance peak demonstrates the switching kinetics between the two forms.

3.0 Contact Mechanics

Hertzian contact mechanics (**Eqn. S1**) was used to estimate E^* by fitting the approach curve up to $F_n = 1$ mN (contact pressure, $P \approx 4 - 9$ kPa).

$$F_n = \frac{4}{3} E^* R^{1/2} d^{3/2} \qquad \text{Eqn. S1}$$

R is the probe radius, F_n is the applied normal force, d is the indentation depth, and $E^* = E/(1-\upsilon^2)$, where E is the compressive elastic modulus and υ is the hydrogel Poisson's ratio.

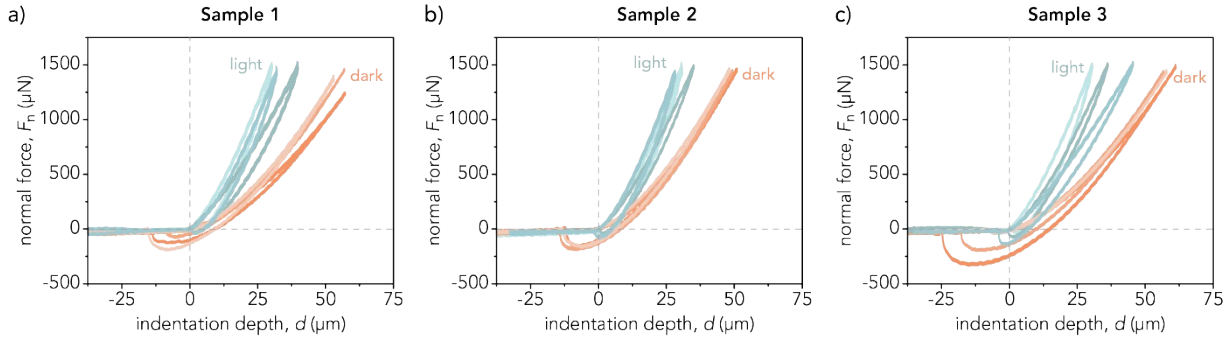

Figure S11 Representative indentation curves for each p(NIPAAm-*co*-AMPS-*co*-SP) hydrogel in the dark and light state for each cycle.

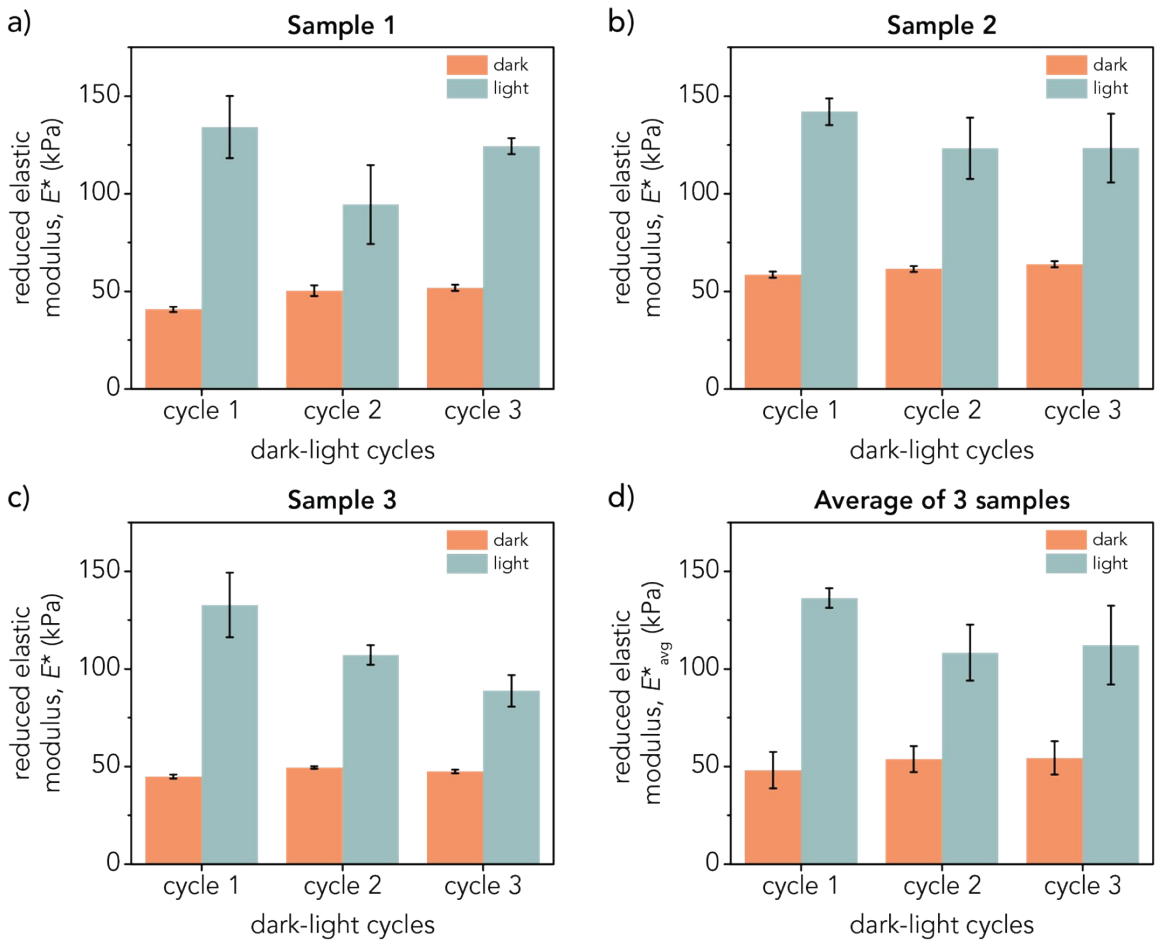

Figure S12 (a-c) Bar charts of reduced elastic modulus for three p(NIPAAm-*co*-AMPS-*co*-SP) hydrogels in the dark and light state for each cycle. Bars represent the averages and standard deviations of 15 indentations. **(d)** Averaged reduced elastic modulus of the three hydrogels for each dark-light cycle.

4.0 Timelapse Videos

Video S1 Timelapse of p(NIPAAm-*co*-AMPS-*co*-SP) hydrogel demonstrating conversion of MCH^+ to SP, indicated by the color change from red-orange to light orange as light penetrates through the top of the hydrogel. Images were taken every 5 sec.

5.0 Hydrogel Volume

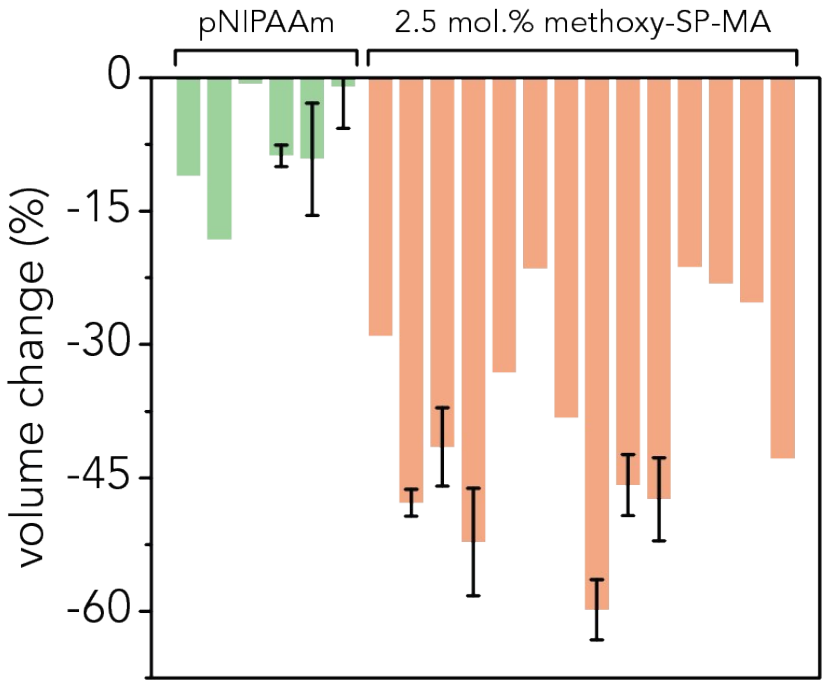

Figure S13 Volume change ((($V_{light,1} - V_{dark,1}$)/$V_{dark,1}$) x 100%) after three hours of 470 nm light irradiation for 20 hydrogels (6 pNIPAAm hydrogels, 14 p(NIPAAm-*co*-AMPS-*co*-SP) hydrogels). Average volume change for pNIPAAm hydrogels: -8 ± 7%. Average volume change for p(NIPAAm-*co*-AMPS-*co*-SP) hydrogels: -38 ± 12%. Error bars come from standard deviation in volume measurements taken with calipers.

6.0 Friction Coefficients

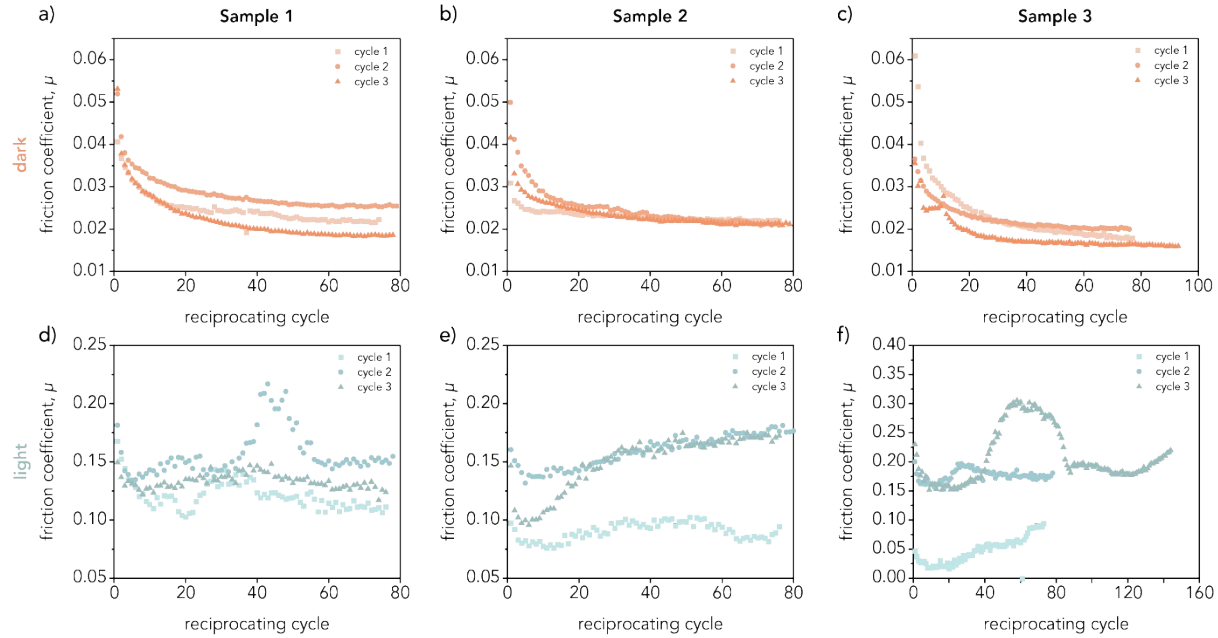

Figure S14 Friction coefficient as a function of reciprocation cycle **(a-c)** in the dark and **(d-f)** under 470 nm irradiation for three hydrogel samples. The last 50 cycles were averaged to obtain μ_{dark} and μ_{light}.

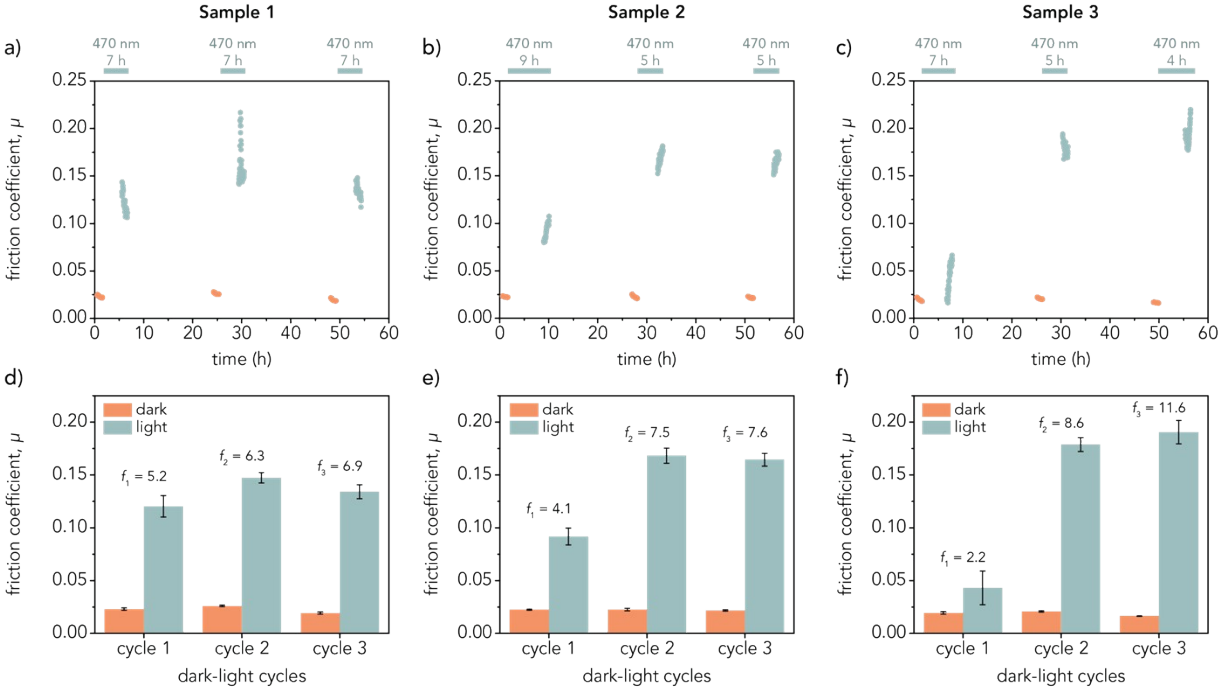

Figure S15 (a-c) Friction coefficient as a function of time and **(d-f)** bar charts for three p(NIPAAm-*co*-AMPS-*co*-SP) hydrogels in the dark and light state for each cycle. Bars represent the averages and standard deviations of 50 friction cycles.

7.0 pNIPAAm

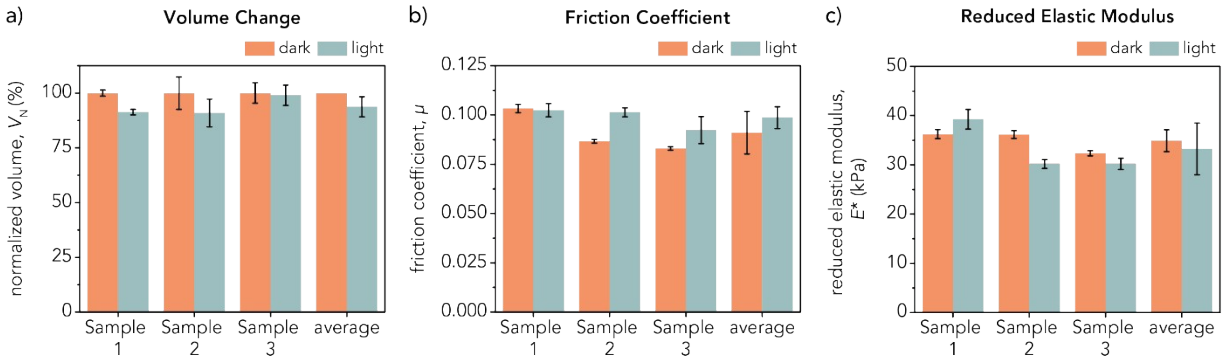

Figure S16 Bar charts of **(a)** normalized volume (($V/V_{dark,1}$) x 100%), **(b)** friction coefficient, and **(c)** reduced elastic modulus for p(NIPAAm) hydrogels before and after 470 nm irradiation for 3 h at 35 ± 1 mW/cm^2. Even though no SP-MA was incorporated into the network, there was still a slight volume change. However, there is no statistically significant change in friction, indicating that the driving force behind the friction change for the p(NIPAAm-*co*-AMPS-*co*-SP) hydrogels are the methoxy-SP-MA incorporated monomers.

8.0 Silanized Hydrogels

Stock solutions of 5 vol.% (3-aminopropyl)triethyoxysilane (APTES) and 5 vol.% glutaraldehyde were prepared with ultrapure water. Glass slides were cleaned with a solution of soap and water, isopropanol, and then submerged in a 10 M NaOH solution overnight. The slides were rinsed with ultrapure water before submersion in 5 vol.% APTES for 40 min and 5 vol.% glutaraldehyde for 30 min. After a final rinse with ultrapure water, the slides were dried with a nitrogen gun. A rubber spacer (0.8 mm thick) was used to separate the silanized glass from an unsilanized glass slide, and a precursor solution of p(NIPAAm-*co*-AMPS-*co*-SP) was polymerized between the slides. After polymerization, the gels were swollen in 100 mM phosphate buffer solution.

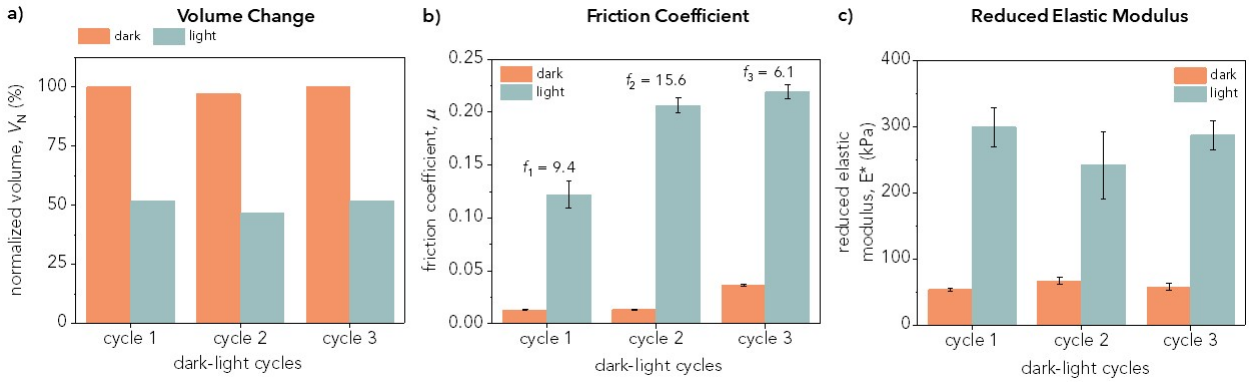

Figure S17 (a) Volume change, **(b)** friction coefficient, and **(c)** reduced elastic modulus for p(NIPAAm-*co*-AMPS-*co*-SP) hydrogels covalently attached to a glass slide on one side. Despite being constrained to swelling in one direction, the volume decreased significantly upon irradiation, leading to large changes in friction coefficient and elastic modulus.

9.0 References

1 L. Wimberger, S. K. K. Prasad, M. D. Peeks, J. Andreásson, T. W. Schmidt and J. E. Beves, *J Am Chem Soc*, 2021, **143**, 20758–20768.

2 C. Li, A. Iscen, L. C. Palmer, G. C. Schatz and S. I. Stupp, *J Am Chem Soc*, 2020, **142**, 8447–8453.

3 J. R. Hemmer, S. O. Poelma, N. Treat, Z. A. Page, N. D. Dolinski, Y. J. Diaz, W. Tomlinson, K. D. Clark, J. P. Hooper, C. J. Hawker and J. Read de Alaniz, *J Am Chem Soc*, 2016, **138**, 13960–13966.